New York State Energy Research and Development Authority

Disposing of Greenhouse Gases through Mineralization Using the Wollastonite Deposits of New York State

Final Report

May 2012

No. 12-14

nyserda
Energy. Innovation. Solutions.

NYSERDA's Promise to New Yorkers:

New Yorkers can count on NYSERDA for objective, reliable, energy-related solutions delivered by accessible, dedicated professionals.

Our Mission: Advance innovative energy solutions in ways that improve New York's economy and environment.

Our Vision: Serve as a catalyst—advancing energy innovation and technology, transforming New York's economy, and empowering people to choose clean and efficient energy as part of their everyday lives.

Our Core Values: Objectivity, integrity, public service, and innovation.

Our Portfolios

NYSERDA programs are organized into five portfolios, each representing a complementary group of offerings with common areas of energy-related focus and objectives.

Energy Efficiency & Renewable Programs

Helping New York to achieve its aggressive clean energy goals – including programs for consumers (commercial, municipal, institutional, industrial, residential, and transportation), renewable power suppliers, and programs designed to support market transformation.

Energy Technology Innovation & Business Development

Helping to stimulate a vibrant innovation ecosystem and a clean energy economy in New York – including programs to support product research, development, and demonstrations, clean-energy business development, and the knowledge-based community at the Saratoga Technology + Energy Park®.

Energy Education and Workforce Development

Helping to build a generation of New Yorkers ready to lead and work in a clean energy economy – including consumer behavior, youth education, and workforce development and training programs for existing and emerging technologies.

Energy and the Environment

Helping to assess and mitigate the environmental impacts of energy production and use – including environmental research and development, regional initiatives to improve environmental sustainability, and West Valley Site Management.

Energy Data, Planning and Policy

Helping to ensure that policy-makers and consumers have objective and reliable information to make informed energy decisions – including State Energy Planning, policy analysis to support the Regional Greenhouse Gas Initiative, and other energy initiatives; and a range of energy data reporting including *Patterns and Trends*.

Disposing of Greenhouse Gases through Mineralization Using the Wollastonite Deposits of New York State

Final Report

Prepared for the
New York State Energy Research and Development Authority

nyserda
Energy. Innovation. Solutions.

Albany, NY
nyserda.ny.gov

Amanda D. Stevens
Project Manager

Prepared by:
Columbia University
Department of Earth and Environmental Engineering, Lenfest Center

Klaus S. Lackner

Ah-Hyung Alissa Park

Huangjing Zhao

NYSERDA
Report 12-14

NYSERDA 10114

May 2012

NOTICE

This report was prepared by Klaus S. Lackner and Ah-Hyung Alissa Park, at Columbia University, in the course of performing work contracted for and sponsored by the New York State Energy Research and Development Authority (hereafter NYSERDA). The opinions expressed in this report do not necessarily reflect those of NYSERDA, or the State of New York. Moreover, reference to any specific product, service, process or method does not constitute an implied or expressed recommendation or endorsement of it. Further, NYSERDA, the State of New York, and the contractor make no warranties or representations, expressed or implied, as to the fitness for particular purpose or merchantability of any product, apparatus, or service, or the usefulness, completeness or accuracy of any processes, methods or other information contained, described, disclosed or referred to in this report. NYSERDA, the State of New York and the contractor make no representation that the use of any product, apparatus, process, method or other information will not infringe privately-owned rights and will assume no liability for any loss, injury or damage resulting from, or occurring in connection with, the use of information contained, described, disclosed or referred to in this report.

Abstract:

Recently, carbon mineralization has received much attention as one of the most promising options for CO_2 sequestration. Carbon mineralization has unique advantages, such as the abundance of naturally occurring calcium- and magnesium-bearing minerals and the formation of environmentally benign and stable carbonates via a thermodynamically favored mechanism. However, several challenges need to be overcome to successfully deploy this technology. In particular, acceleration of the extremely slow weathering step, along with process optimization, is essential to ensure economic feasibility. In this study, the effect of various types of chelating agents on the dissolution rate of wollastonite, a calcium-silicate mineral, was explored to accelerate the weathering rate. Wollastonite was chosen because the largest deposits of wollastonite in the U.S. exist in New York State. It was observed that chelating agents, such as acetic acid and gluconic acid, which bind Ca^{2+} from the mineral, significantly improved the dissolution kinetics of wollastonite, even at a diluted concentration of 0.006 M. Calcium extracted from wollastonite was then reacted with CO_2 to form precipitated calcium carbonate (PCC) that mimics commercially available $CaCO_3$-based filler materials. The particle size distribution and the morphological structures of synthesized PCC were investigated as functions of reaction time, pH, and reaction temperature.

Keywords: CO_2 mineralization, wollastonite, mineral dissolution, chelating agents, carbonation, precipitated calcium carbonate, sequestration

Acknowledgments

The work presented in this report was funded by New York State Energy Research and Development Authority (Agreement Number: 10114).

Table of Contents

Summary **S-1**

1 Introduction **1**

2 Materials and Methods **5**

2.1 Wollastonite 5

2.2 Mineral Dissolution 6

2.3 Formation of Calcium Carbonate 8

3 Results and Discussion **9**

3.1 Mineral Dissolution 9

3.2 Formation of Calcium Carbonate 13

3.2.1 Effects on Particle Size 13

3.2.2 Effects on Morphological Structure 15

3.2.3 Effects of Different Calcium Sources on Synthesis of Precipitated Calcium Carbonate 17

4 Thermodynamic Modeling and Flow Diagram of Industrial Process **21**

4.1 Thermodynamic Modeling 21

4.2 Flow Diagram of Industrial Process 23

References **25**

Listing of Tables and Figures

Table 1. List of chelating agents and their stability constants (β) with Ca^{2+}.....11

Figure 1. Examples of commercially available precipitated calcium carbonate morphologies. 3
Figure 2. Particle-size distribution and SEM image of the ground wollastonite particles. 5
Figure 3. XRD patterns and Rietveld refined fits (R_{wp} = 14.1%) of wollastonite. Inset illustrates the crystal structure of wollastonite 1A..... 6
Figure 4. Schematic diagram of experimental setup for mineral dissolution. 7
Figure 5. (a) [Ca_{total}] in liquid samples from the differential bed reactor, where [Ca_{total}] = [Ca^{2+}] + [CaL] (L=ligand) and (b) Ca extraction as a function of time at 25 °C. 10
Figure 6. Comparison of Ca extraction from wollastonite using various chelating agents (25 °C, reaction time = 6 min). 11
Figure 7. Speciation of various chelating agents, as a function of pH, simulated using Visual MINTEQ: (a) 0.006 M acetic acid, (b) 0.003 M oxalic acid, (c) 0.002 M citric acid, and (d) 0.0015 M EDTA. 12
Figure 8. Effect of ligand concentrations on wollastonite dissolution (25 °C, reaction time = 6 min). 13
Figure 9. Mean particle size (a) and particle-size distributions (b) of $CaCO_3$, synthesized using model Ca-solution as a function of aging time at 295 K. 14
Figure 10. Mean particle size (a) and particle-size distributions (b) of $CaCO_3$, synthesized using model Ca-solution as a function of reaction temperature (aging time = 30 min). 14
Figure 11. Mean particle size (a) and particle-size distributions (b) of $CaCO_3$, synthesized using model Ca-solution as a function of pH at 295 K (aging time = 30 min, pH was measured after the precipitation) 15
Figure 12. SEM images of $CaCO_3$ synthesized using model Ca-solution at various pH conditions (reaction temperature = 295 K, aging time= 30 min). 16
Figure 13. SEM images of $CaCO_3$ synthesized using model Ca-solution at various temperature conditions (aging time =30 min). 16
Figure 14. Comparison of mean particle size (a) and particle-size distributions (b) of $CaCO_3$, synthesized using wollastonite and model Ca-solution at 295 K and 355 K (aging time = 30 min).....17
Figure 15. Rietveld refinement results of $CaCO_3$ synthesized with wollastonite and $Ca(NO_3)_2$ at (a) 295 K and (b) 355 K. Insets indicate crystalline structures of vaterite, calcite, and aragonite. 18

Figure 16. SEM images of $CaCO_3$ synthesized with $Ca(NO_3)_2$ ((a) and (c)) and wollastonite ((b) and (d)) at two temperature conditions of 295 K and 355 K with different magnifications. 19
Figure 17. TGA results of $CaCO_3$ synthesized with wollastonite and $Ca(NO_3)_2$ at 295 K and 355 K. 19
Figure 18. Effect of the partial pressure of CO_2 on wollastonite dissolution at 120 ºC. 21
Figure 19. Effect of the partial pressure of CO_2 on precipitation of calcium carbonate at 120 ºC 22
Figure 20. Effect of temperature on wollastonite dissolution at P_{CO2} = 40 bars. 22
Figure 21. Effect of temperature on precipitation of calcium carbonate at P_{CO2} = 40 bars. 23
Figure 22. Sketch of flow diagram of the industrial carbon-mineralization process 23

Summary

Carbon mineralization is one of the safest methods of sequestering anthropogenic carbon dioxide. It is based on the exothermic reaction between carbon dioxide and the metal ions present in silicate minerals to form geologically and thermodynamically stable mineral carbonates. Most of the silicate minerals available for carbon mineralization are rich in magnesium (e.g., serpentine and olivine). Thus, recent research has been aimed at the accelerated weathering of Mg-bearing silicate minerals. However, the selection of minerals appropriate for carbon storage is highly location-specific due to the potentially large transportation cost. Therefore, other minerals in smaller scales should also be investigated for their carbon-storage potential.

This study focuses on the dissolution and carbonation of wollastonite. Since the largest deposits of wollastonite in the U.S. exist in New York State, where limited carbon-storage options are available, the fixation of anthropogenic CO_2 into mineral carbonates could be one of the best options for the state. It is estimated that there are 7-14 Mt of wollastonite in New York; this translates to a storage potential of 2-5 million tons of CO_2. Thus, New York is in a strong position to demonstrate the viability of mineral sequestration on wollastonite minerals, which are easier to carbonate than olivine and serpentine. Not only is the carbonation easier with wollastonite, but also the mining infrastructure that is required for processing the minerals has already been built and is operating commercially.

The overall chemical process by which the calcium from wollastonite is carbonated can be separated into two steps: dissolution and carbonation. In the dissolution step, effects of various chelating agents on the enhanced dissolution of wollastonite were investigated. It was found that the most dissolution of wollastonite occurred in the first few seconds, attributed to the presence of very fine particles. Chelating agents, such as weak organic acids that target and form complexes with Ca in a mineral matrix, improved the dissolution kinetics of wollastonite by orders of magnitude, even at concentrations as low as 0.006 M. The effect of a wide variety of chelating agents on wollastonite dissolution was determined. Dissolution studies revealed that gluconic acid, citric acid, and acetic acid are better than other chelating agents. As expected, the mineral-dissolution rate was enhanced by increasing the concentration of chelating agents.

The dissolved calcium ions were then carbonated to form precipitated calcium carbonate (PCC), which mimics commercially available $CaCO_3$-based filler materials. First, the particle-size distribution and the morphological structures of synthesized PCC were investigated, as functions of reaction time, pH, and reaction temperature with model Ca-solution (calcium nitrate). Then, soluble Ca species extracted from wollastonite were used to form carbonate and compared with the one synthesized with pure chemical. A comparison between PCC synthesized from wollastonite and $Ca(NO_3)_2$ revealed that the morphological and crystal structures were identical, but the particle-size distributions were slightly different because of the chelating agents used in the dissolution step. Finally, the structures and particle-size distribution could be controlled by changing reaction parameters, such as temperature and pH.

1 Introduction

Carbon dioxide is one of the greenhouse gases known to cause climate change.[1-3] Significant increases in the concentration of atmospheric carbon dioxide are also changing the surface chemistry of the ocean, leading to other detrimental environmental impacts, including the acidification of the ocean. Reducing the increasing levels of anthropogenic CO_2 in the atmosphere is one of the most significant concerns in energy- and environmental-research areas.[1,2] Efforts to develop renewable energy sources and improve efficiency of energy production and use are underway to reduce CO_2 emissions. However, given the rising global demand for energy and increasing consumption of fossil fuels, CO_2 capture and sequestration (CCS) technologies are necessary to curb CO_2 emissions.[4] Various schemes have been proposed and developed for efficient CO_2 capture and sequestration.[5,6] In particular, many sequestration options have been investigated, including geological storage,[7,8] ocean storage,[9,10] and mineral sequestration[11–14]. Currently, geological storage of CO_2 is considered to be the most economical method for sequestration, while CO_2 sequestration by forming mineral carbonates is relatively new and less explored.

CO_2 mineral sequestration involves exothermic carbonation of naturally occurring Mg- or Ca-bearing silicate minerals, such as serpentine ($Mg_3Si_2O_5(OH)_4$), forsterite/olivine ($Mg_2Si_2O_4$), or wollastonite ($CaSiO_3$). The well-recognized advantages of CO_2 mineralization can be summarized as (i) very large capacity, (ii) no necessity of monitoring after disposal, and (iii) environmentally benign and thermodynamically stable products. Thus, this option facilitates permanent removal of CO_2 from the atmosphere. However, the slow chemistry of the reaction − natural weathering occurs on geological time-scales − is still a major issue in the process of CO_2 mineralization.

Since the concept of mineral sequestration for CCS was first illustrated by Seifritz in 1990,[11] more-detailed methods have been proposed, including an aqueous scheme[15] and an underground-injection method[16]. Direct carbonation of Mg-bearing silicate minerals, such as serpentine, was first attempted in a gas/solid process at high-pressure and high-temperature conditions (500 °C and 340 bar) by Butt et al., showing relatively slow conversion rate.[17] Lackner, et al. also proposed an indirect mineral-carbonation process to produce a more reactive form of magnesium, via $MgCl_2$, in a separated step.[18] While indirect processes offer relatively fast reaction kinetics and better product quality, reaction pathways are too complex and energy intensive.[19,20] Since a direct-carbonation scheme in aqueous solution was developed by O'Connor et al.,[21–23] significant attempts have been made in both direct- and indirect-carbonation schemes, including the extraction of Mg or Ca from silicate minerals using chemical additives, such as salts, acids, alkali solutions, or ligands.[24–27] It has been known that the process parameters, such as pH, temperature, pressure, and particle-size distribution, significantly affect the reaction kinetics in mineral carbonation.[28,29] Park and Fan also investigated the effect of the physical activation on the dissolution of serpentine mineral with a pH-swing scheme to enhance mineral carbonation.[25] The pH-swing process is beneficial in that high-purity iron oxide and $MgCO_3$ are produced as value-added products, potentially reducing the overall cost of

the carbon-sequestration process. The effects of weak organic acids and additives in enhancing mineral-dissolution kinetics were also reported.[30,31]

For large-scale CO_2 sequestration via carbon mineralization, generally Mg-bearing silicate minerals, such as serpentine or forsterite/olivine, are the most suitable minerals, due not only to their significant abundance in nature, but also their high capacity.[5] For example, the theoretical CO_2-binding capacity (R_{CO2}) for serpentine is 2.1 ton-mineral/ton-CO_2, whereas R_{CO2} is 2.6 ton-mineral/ton-CO_2 for wollastonite.[32,33] Thus, research on CO_2 mineralization has been more focused on magnesium-silicate minerals than calcium-silicate minerals, such as wollastonite. Nonetheless, Ca-based silicate materials have a significant potential for utilization in CO_2 sequestration. Because the choice for optimal CO_2 sequestration largely depends on regional conditions in connection with CO_2 transportation, CO_2 mineralization via Ca-bearing minerals could be a plausible option in specific areas where Ca-bearing silicates are largely deposited. The world reserves of wollastonite are estimated to exceed 90 million tons (probable reserves estimated to be 270 million tons),[34] with large reserves in China, Finland, India, Mexico, Spain, and the U.S.[35] In addition, the abundance of Ca in basalt rock (~9.4 wt% CaO) offers additional potential.[21] Moreover, the technologies developed for enhancing carbonation of Ca-bearing minerals can also be applied to the carbonation of industrial wastes, such as steel slag and cement kiln dust, which contain a significant amount of calcium.[36–39]

Good sites for underground injections are rare, and options for enhanced oil recovery are virtually nonexistent in the State of New York (although enhanced gas recovery may yet be an option). The largest deposits of wollastonite in the U.S., however, exist in Essex and Lewis counties of New York State. The deposits are currently being mined by the NYCO and R.T. Vanderbilt mining companies. The ore bodies mined by NYCO contain wollastonite, garnet, and diopside. Parts of them contain up to 60% wollastonite. The ore bodies mined by R.T. Vanderbilt contain primarily wollastonite, as well as minor amounts of calcite and prehnite and trace amounts of diopside. It is estimated that New York State's production of wollastonite ranges between 115,000 to 127,000 tons per year, and there is 7-14 Mt of wollastonite total, which, theoretically, can store 2-5 million tons of carbon dioxide.[40] Thus, New York is in a strong position to demonstrate the viability of mineral sequestration on wollastonite minerals, which are easier to carbonate than the olivine and serpentine minerals. Not only is the carbonation easier with wollastonite, but also the mining infrastructure required for processing the minerals has already been built and is operating commercially.

The overall chemical process by which the calcium from wollastonite is carbonated can be separated into two stages. First is the dissolution of calcium from the mineral into solution, and second is the precipitation of calcium carbonate from solution. When mineral dissolution and carbonation take place simultaneously in an aqueous solution, the process is known as the direct-carbonation approach.[22] Using this approach, the entire process is thermodynamically favored. As a result, energy inputs are not required during the chemical processing of the material. This method is currently regarded as the most economical mineral-carbonation pathway.

However, there are two aspects of the direct-carbonation process that are not yet optimized with respect to reaction kinetics. First, by combining the dissolution and carbonation steps into one single batch process, one must compromise with the solution pH, pressure, and temperature conditions to accommodate both steps. The optimal conditions for the carbonate precipitation reaction (low acidity, low temperature) are opposite to that of the silicate-dissolution reaction (high acidity, high temperature). By separating the dissolution and carbonation steps, optimal conditions may be tailored to each step separately, thereby increasing the overall reaction kinetics. Second, potential chelating agents and catalysts have been relatively unexplored for use in mineral dissolution and carbonation processes.

Due to the relatively high cost ($50-$100/net ton of CO_2 sequestered) associated with carbon mineral sequestration, a breakthrough in this technology will not be possible without considering the utilization of solid products.[2,22] During carbon mineral sequestration using wollastonite, $CaCO_3$, which is widely used commercially, is produced. The demand for precipitated calcium carbonate (PCC) is enormous in the paper, paints, and plastics/rubber industries.[41,42] Appropriate filler materials provide paper with desirable physical and optical characteristics, including improved dry strength, smoothness, and brightness. The ability to control the size, morphology, and uniformity is paramount for filler materials, and thus, PCC has become the preferred filler of choice over alternatives, such as ground calcium carbonate.[43] For that objective, calcium carbonate was synthesized with tailored properties, such as mean particle size, particle size distribution and surface morphology, to emulate some commercially made PCC particles, which are shown in Figure 1,[44] during carbon mineral sequestration.

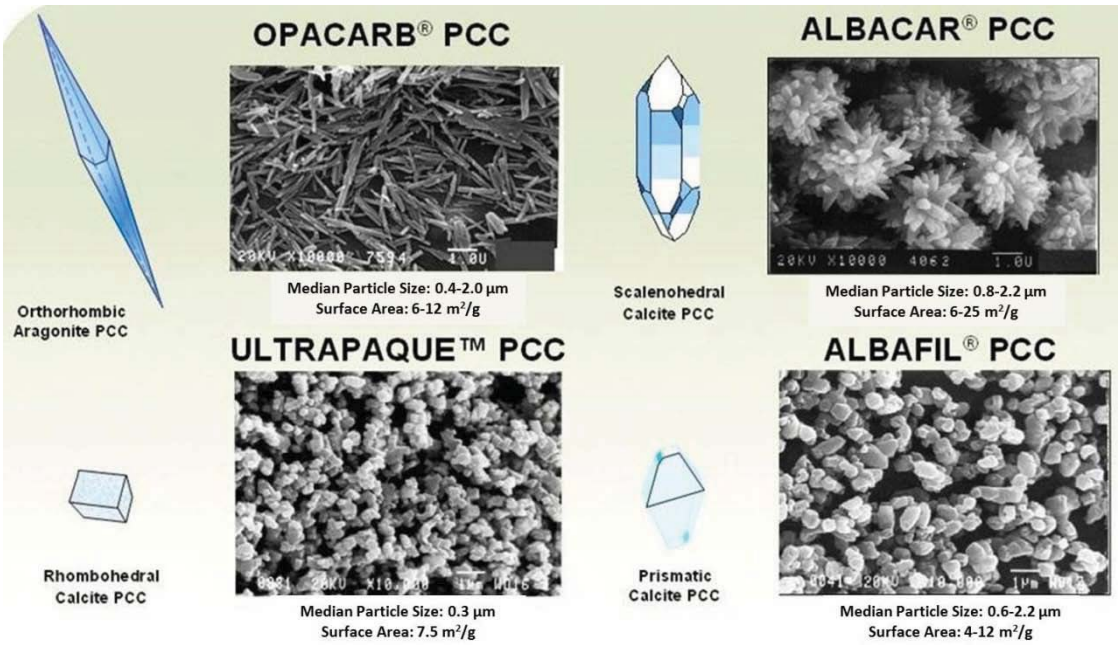

Figure 1. Examples of commercially available precipitated calcium-carbonate morphologies.

This report illustrates the effects of various types of chelating agents on the dissolution of wollastonite to accelerate and optimize the weathering kinetics. The indirect-mineralization scheme presented in this study also includes the formation of PCC as a result of CO_2 reacting with the extracted calcium. The synthesized PCC was tailored with properties such as a desired particle-size distribution and surface morphology by controlling reaction time, temperature, and pH.

2 Materials and Methods

2.1 Wollastonite

Minerals mined by R.T. Vanderbilt Co., Inc. were chosen for this study. These minerals also contained small amounts of calcite, prehnite, and trace amounts of diopside. These wollastonite samples were mostly mining tailings with a large particle-size distribution. Since a uniform particle size is desirable for the kinetic studies, wollastonite samples were sent to SGS Minerals Ltd. in Canada to be ground and prepped.

For the further experiments, the ground wollastonite samples were sieved to collect fine particles, which were smaller than 175 μm. The particle-size distribution was obtained through laser diffraction measurement (LS^{TM} 13 320 MW, Beckman Coulter, Inc., Brea, CA), and the results are shown in Figure 2; the average particle size for fine wollastonite sample was 108.59 μm. Although the sieving method is the simplest and most energy efficient way to obtain fine particles, it was found that this method is not suitable for larger wollastonite particles. The particle size was underestimated, due to its high aspect ratio and acicular shape. The morphological structure of wollastonite was investigated using Scanning Electron Microscopy (SEM, JSM-5600 LV, JEOL Ltd., Tokyo, Japan). As shown in Figure 2, the shapes of wollastonite particles were irregular, and the broken edges were very sharp.

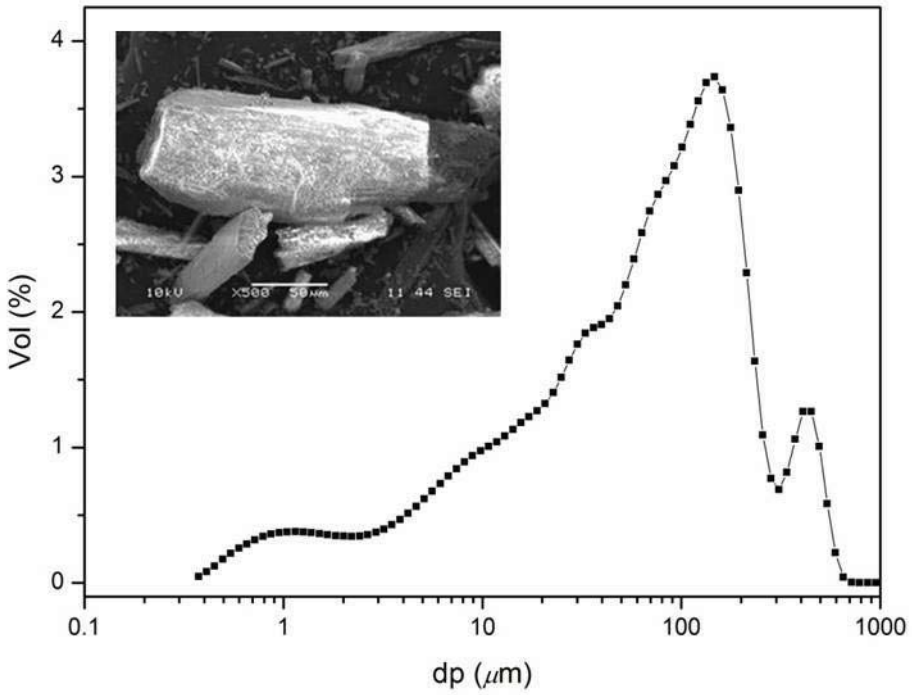

Figure 2. Particle-size distribution and SEM image of the ground wollastonite particles.

For the information of crystalline structures in the sample, an X-ray diffractometer (XRG 3000, Inel Inc., Stratham, NH) was employed. The powder X-ray diffraction (XRD) patterns were obtained in the 2θ range of 20-60° at room temperature, using CuKα radiation (λ = 1.5406Å). In order to analyze the crystalline structures in the sample and the corresponding composition, a Rietveld refinement method was used via MAUD (Material Analysis Using Diffraction) package.[45] The powder XRD pattern was obtained and the spectrum with Rietveld refinement fits is shown in Figure 3. The ground powder mainly contains wollastonite (Wollastonite 1A, space group: $P\bar{1}$, a = 7.963 Å, b = 7.350 Å, c = 7.034 Å, α = 90.73°, β = 95.10°, γ = 104.92°) with small amounts of wollastonite 2M (parawollastonite, space group: $P2_1$, a = 15.409 Å, b = 7.322 Å, c = 7.063 Å, β = 95.30°) and quartz. It was found that the Ca-element concentration was 27.0 wt% in the wollastonite minerals, as measured by ICP-OES via the lithium metaborate-acid dissolution procedure.[46]

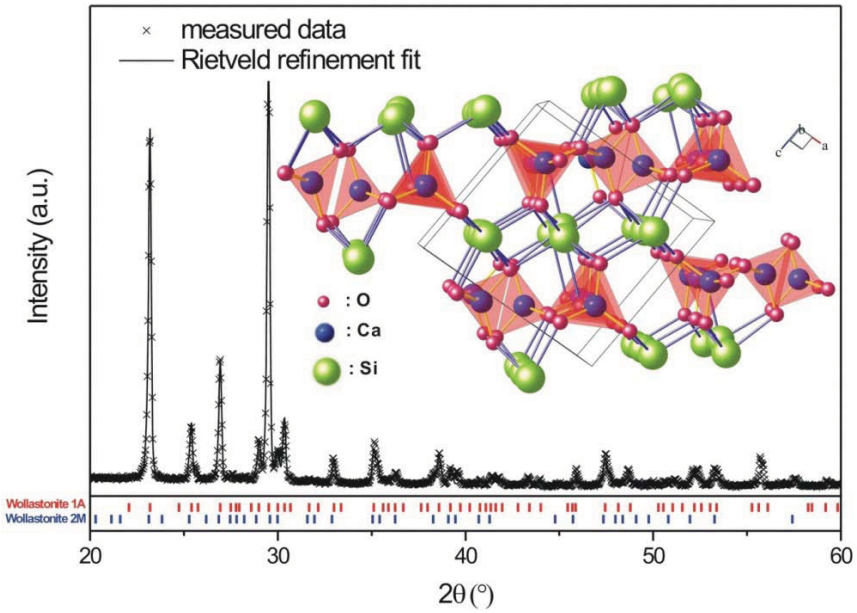

Figure 3. XRD patterns and Rietveld refined fits (R_{wp} = 14.1%) of wollastonite. Inset illustrates the crystal structure of wollastonite 1A.

2.2 Mineral Dissolution

As mentioned earlier, the process method selected for the accelerated carbonation of wollastonite in this study was the indirect aqueous route, in which the dissolution and carbonation steps are decoupled and studied separately, using different reactor configurations. The goal in the dissolution step was to find suitable chelating agents for dissolving wollastonite minerals. For selecting the chelating agents, metal-ligand interactions and positive results from previous studies based on literatures were considered, especially metal-ligand interactions.

In order to investigate the effect of chelating agents on dissolution kinetics, various chelating agents were selected: acetic acid (CH_3COOH), nitrilotriacetic acid (NTA, $C_6H_9NO_6$), picolinic acid ($C_6H_5NO_2$),

iminodiacetic acid (IDA, $HN(CH_2CO_2H)_2$), ethylenediaminetetraacetic acid (EDTA, $C_{10}H_{16}N_2O_8$), gluconic acid ($C_6H_{12}O_7$), phthalic acid ($C_8H_6O_4$), citric acid ($C_6H_8O_7$), ascorbic acid ($C_6H_8O_6$), glutamic acid ($C_5H_9NO_4$), and oxalic acid ($C_2H_2O_4$). All chelating agents were supplied by Sigma-Aldrich Co. LLC (St. Louis, MO).

A differential bed reactor was used to explore the dissolution behavior, using selected chelating agents. A syringe with capacity of 60 ml was used, coupled with a syringe pump (NE-1000, New Ear Pump System Inc., Farmingdale, NY). The solvents containing various chelating agents were prepared and filled in the syringe. The solvents include 0.006 M for monoprotic acids (acetic acid, picolinic acid, and gluconic acid); 0.003 M for diprotic acid (IDA, phthalic acid, ascorbic acid, glutamic acid, and oxalic acid); 0.002 M for triprotic acid (NTA and citric acid); and 0.0015 M for tetraprotic acid (EDTA). A small amount of wollastonite (20 mg) was uniformly distributed in a sample holder, which was then attached to the syringe. The flow rate of the solutions was set to 10 ml/min. Since the wollastonite was always in contact with fresh solvent, buffers were not required in this system. All the reactions were performed at room temperature. The schematic diagram of the reactor is shown in Figure 4.

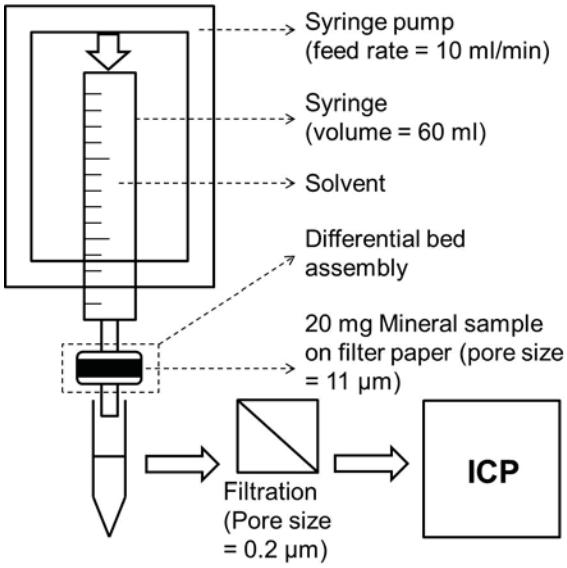

Figure 4. Schematic diagram of experimental setup for mineral dissolution.

The total reaction time was about six minutes for each experimental run. For the elemental analysis, the liquid samples were collected in time intervals of 8-40 seconds (for the first 90 seconds, samples were collected every 8 seconds, and after that samples were collected every 40 seconds). After being filtered (pore size: 0.2 μm), they were analyzed by employing an Inductively Coupled Plasma Optical Emission Spectrometer (ICP-OES: ACTIVA-M, Horiba Jobin Yvon Inc., Edison, NJ). Based on the result in the first test, dissolution behaviors of Ca^{2+} from wollastonite minerals were measured again under higher chelating-agent concentrations for selected acids, such as gluconic acid, citric acid, and acetic acid.

2.3 Formation of Calcium Carbonate

In this part, the pure calcium source, calcium nitrate ($Ca(NO_3)_2$), was used in the carbonation experiments first. Calcium-nitrate solution was employed because it is a simpler calcium source and it is easier to study the effects of pH, reaction time, and reaction temperature on the mean particle size, particle size distribution, thermal stability, and particle morphological structures. 200 ml of 0.25 M K_2CO_3 solution and 100 ml of 0.5 M $Ca(NO_3)_2$ solution were prepared, and mixed in a 500 ml beaker reactor placed in a water bath to achieve the precipitation of calcium carbonate. The mixture was mixed at 800 rpm throughout the experiments, and the samples were periodically (at 5 minutes, 15 minutes, 30 minutes and 60 minutes) collected to determine the particle-size distribution. The reaction temperature was 295 K. The slurry was then filtered and the filter cake was washed with deionized water. The final products, fine white powders, were obtained after drying overnight at room temperature. The final products were then analyzed, using XRD, laser diffraction, SEM, and Thermogravimetric Analyzer (TGA, Q50, TA Instruments Inc., New Castle, DE). The precipitation experiments were repeated at 315 K, 335 K, and 355 K, but samples were collected only one time, at 30 minutes, for the study of effect of reaction temperature on the synthesis of PCC. For the study of effect of pH on the synthesis of PCC, HNO_3 and KOH solutions were used to change the pH condition for the precipitation experiments. The precipitation experiments were repeated at five different pH conditions (pH = 7.92, 8.10, 8.21, 11.67, 12.75). The reaction time for this study was also 30 minutes.

In order to compare the particle-size distribution, thermal stability, and morphological structure of precipitated $CaCO_3$ from wollastonite and pure $Ca(NO_3)_2$, the calcium species extracted from wollastonite by acetic acid were then used to form carbonates. After dissolving wollastonite in acetic acid (1 M), the slurry was filtered and the liquid solution was collected. The pH of the solution (100 ml) was adjusted to the same as the pH of a 0.5 M $Ca(NO_3)_2$ solution. This solution was then added to 0.25 M K_2CO_3 solution and stirred at 800 rpm for 30 minutes to achieve precipitation of $CaCO_3$. These experiments were performed at 295 K and 355 K. The final products were then analyzed using XRD, laser diffraction, SEM, and TGA.

3 Results and Discussion

3.1 Mineral Dissolution

The reaction between the metal ion and chelating agent via ligand interaction can be expressed as

$$\mathrm{mM} + \mathrm{lL} + \mathrm{hH}^{+} \leftrightarrow \mathrm{M_mL_lH_h} \quad (1)$$

where M and L indicate metal ion species and chelating agent, respectively. Thus, it is expected that the extracted calcium species in aqueous solution from wollastonite via chelating agent exists as dissolved Ca^{2+} or a complex with chelating agent. Because pH plays a most significant role in the dissolution process, each dissolution reaction was first performed under similar pH conditions. In order to control the pH, the concentration of each chelating agent was adjusted to 0.006 M, 0.003 M, 0.002 M, and 0.0015 M for monoprotic, diprotic, triprotic, and tetraprotic acid, respectively. Figure 5 (a) shows the total concentration of extracted calcium from the wollastonite. There was a rapid decrease in the dissolution rate in the first few seconds. This is due to the dissolution of very fine particles (< 5 μm), which have a very high surface area. The reaction time for the dissolution experiments was around six minutes. The conversion ratio for each chelating agent was calculated using the equation

$$\text{Conversion } (\%) = \frac{M_\mathrm{d}}{M_\mathrm{m}} \times 100 \quad (2)$$

where M_d and M_m indicate the total dissolved calcium as either form of Ca^{2+} or bound calcium to chelating agents, and calcium in the wollastonite mineral, respectively. Ca^{2+} and calcium complexes are both candidates that can react with CO_3^{2-} to form calcium carbonates in the precipitation step. The ICP measured the concentration of calcium dissolved in the solution, which is the same as total calcium concentration. Figure 5 (b) shows the conversion (%). Calcium extraction from wollastonite was enhanced in the presence of all chelating agents except oxalic acid.

Figure 6 represents the overall conversion ratio at six minutes with pH conditions of the solutions. pH has a significant effect on calcium extraction. Calcium extraction is enhanced by solutions at low pH containing chelating agents, compared with deionized water at low pH. Interestingly, oxalic acid, which shows a pH value of ~ 2.7, exhibits the lowest conversion ratio among chelating agents, similar to the dissolution rate in water. Oxalic acid does not work well for enhancing the dissolution of wollastonite because the solubility of calcium oxalate, which is the primary complex formed in the reaction between calcium ion and oxalate ion, is very low. Consequently, calcium oxalate precipitates out during the dissolution of wollastonite.

The differences in calcium-dissolution behavior among the chelating agents were also observed. Specific chelating agents, such as acetic acid, NTA, and picolinic acid, possess relatively enhanced conversion rates, compared with others. Even at relatively higher pH values, acetic acid (pH ~ 3.5) and picolinic acid (pH ~ 3.9) significantly improved the dissolution rate. These features imply that the physicochemical nature of chelating agents plays an important role in the dissolution reaction, as well as the pH condition. Generally, chelating agents exist in various protonated forms in aqueous solutions with

distributions depending on pH, and each form shows different binding power for calcium species.[47] Table 1 shows the properties of various chelating agents with Ca^{2+}. [48]

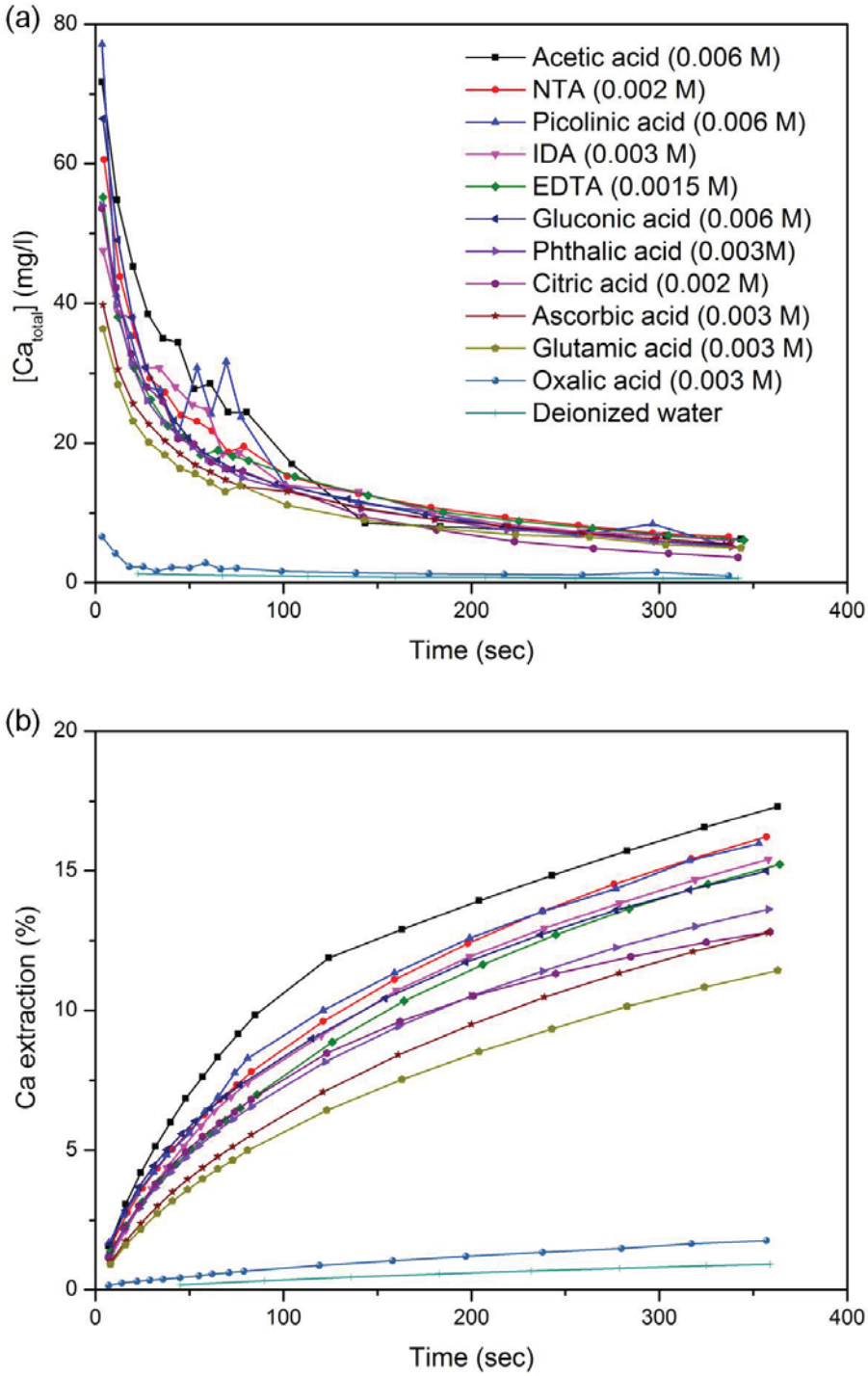

Figure 5. (a) $[Ca_{total}]$ in liquid samples from the differential bed reactor, where $[Ca_{total}] = [Ca^{2+}] + [CaL]$ (L=ligand) and (b) Ca extraction as a function of time at 25 °C.

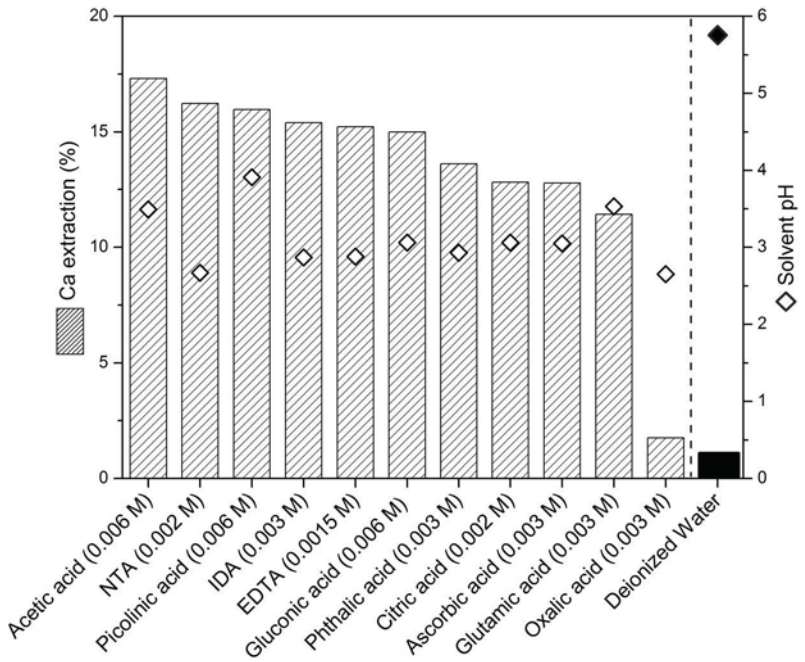

Figure 6. Comparison of Ca extraction from wollastonite using various chelating agents (25 °C, reaction time = six min).

Table 1. List of chelating agents and their stability constants (β) with Ca^{2+}.

Ligands	Molecular formula	Complex	Log β
Ascorbate	$C_6H_6O_6^{2-}$	CaL	0.19
Acetate	$C_2H_3O_2^-$	CaL^+	1.2
Gluconate	$C_6H_{11}O_7^-$	CaL_2	1.21
Glutamate	$C_5H_7NO_4^{2-}$	CaL	2.1
Phthalate	$C_8H_4O_4^{2-}$	CaL	2.4
Oxalate	$C_2O_4^{2-}$	CaL	3.2
IDA	$C_4H_5NO_4^{2-}$	CaL	3.5
Picolinate	$C_6H_4NO_2^-$	CaL^+ CaL_2	2.2 3.8
NTA	$N_6H_6NO_6^{3-}$	CaL^-	7.6
Citrate	$C_6H_5O_7^{3-}$	CaL^- CaHL CaH_2L^+	4.7 9.5 12.3
EDTA	$C_{10}H_{12}N_2O_8^{4-}$	CaL^{2-} $CaHL^-$	12.4 16

In order to check the distributions of the protonated forms of each chelating agent at different pH conditions, activities for each protonated form were simulated as a function of pH (Figure 7). Each protonated form of a chelating agent shows different activities as a function of pH, and has a different stability constant. For example, it was found that the activities of $EDTA^{4-}$ and $HEDTA^{3-}$, which complex with calcium, were very low at a pH of 3 compared with $acetate^{-}$, but because of the high stability constants of the calcium complexes for $EDTA^{4-}$ and $HEDTA^{3-}$, EDTA also works well on enhancing the dissolution of wollastonite. When evaluating the effect of each chelating agent on the dissolution of wollastonite, the activity of the ion that complexes with calcium, the stability constant of the calcium complex formed by that ion and Ca^{2+}, and the solubility of the formed complex should all be considered.

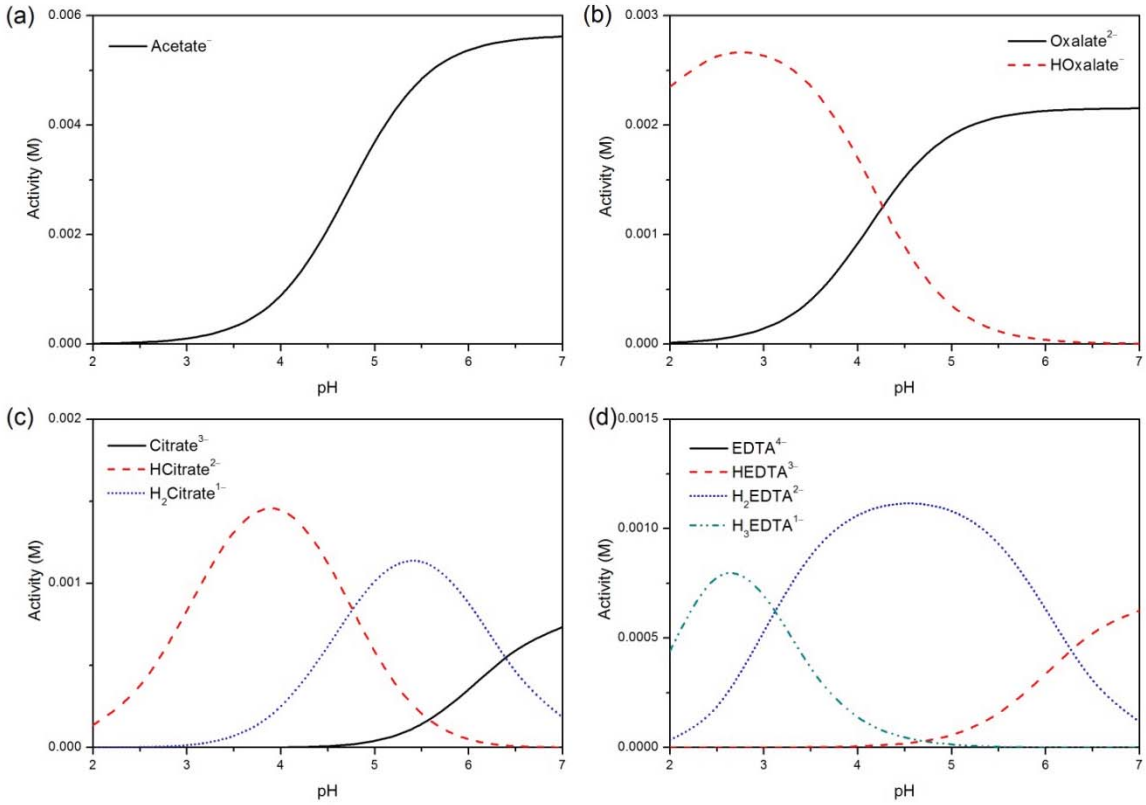

Figure 7. Speciation of various chelating agents as a function of pH, simulated using Visual MINTEQ: (a) 0.006 M acetic acid, (b) 0.003 M oxalic acid, (c) 0.002 M citric acid, and (d) 0.0015 M EDTA.

In order to determine the conversion rates at higher-concentration conditions of chelating agent, selected chelating agents, such as gluconic acid, citric acid, and acetic acid, were prepared with various concentrations. As expected, the conversion rates were increased with increasing concentration of chelating agents (Figure 8).

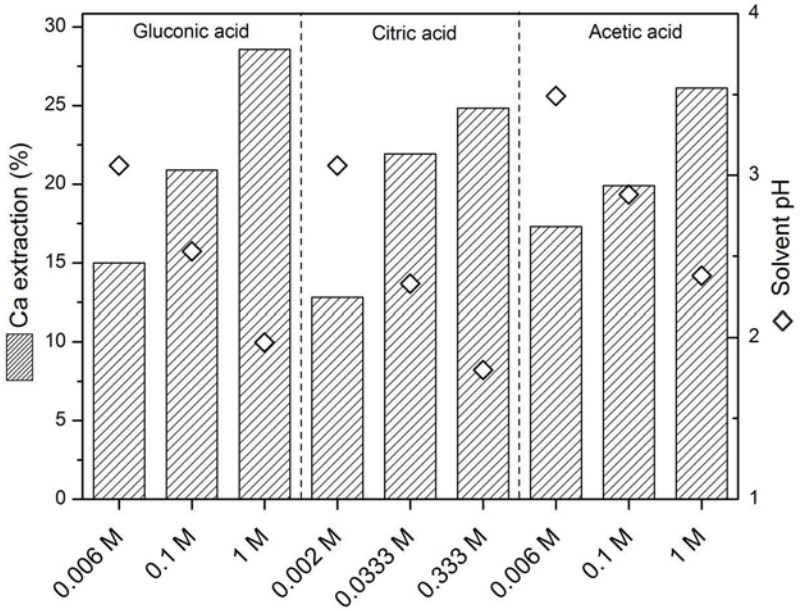

Figure 8. Effect of ligand concentrations on wollastonite dissolution (25 °C, reaction time = six min).

3.2 Formation of Calcium Carbonate

3.2.1 Effects on Particle Size

In the precipitation step, effects of pH, reaction time, and reaction temperature on the mean particle size, particle-size distribution, thermal stability, and particle morphological structures were first studied with a solution of $Ca(NO_3)_2$. As shown in Figure 9, the reaction time did not significantly affect the particle size and particle-size distribution of PCC. The mean particle size of PCC increased slightly as the crystallization process was carried out over a longer period of time. However, the difference was small. On the other hand, the particle-size distributions of PCC that were synthesized under different temperatures had very significant differences (Figure 10). However, it was not easy to find a trend as a function of temperature, due to a change in the particle morphological structure. For example, spherical particles and needle-shaped particles result in different particle size and particle-size distribution. Finally, Figure 11 shows the effect of pH on the mean particle size and particle-size distribution. As the pH of the solution increased, the mean diameter of the produced PCC particles decreased.

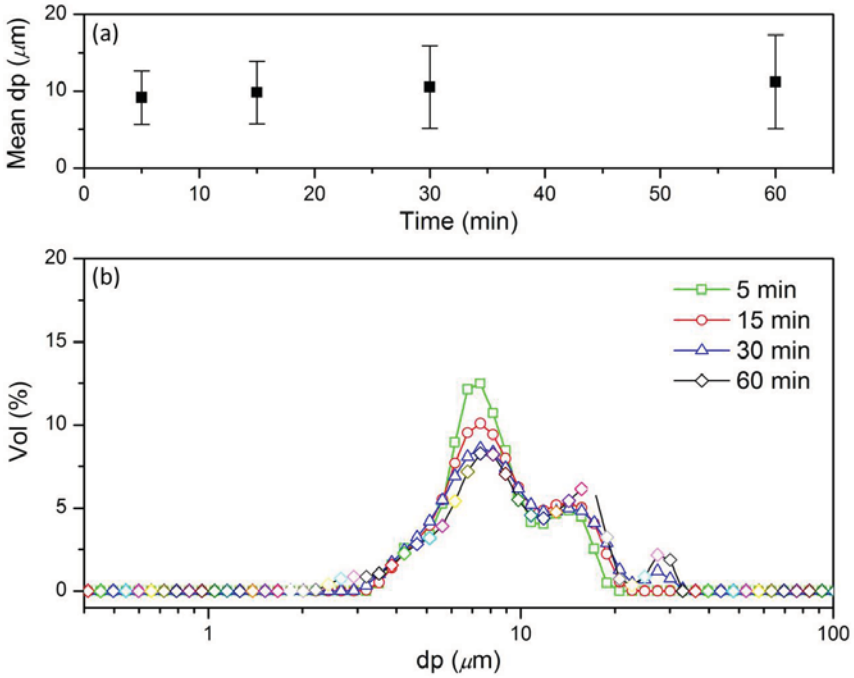

Figure 9. Mean particle size (a) and particle-size distributions (b) of $CaCO_3$, synthesized using model Ca-solution as a function of aging time at 295 K.

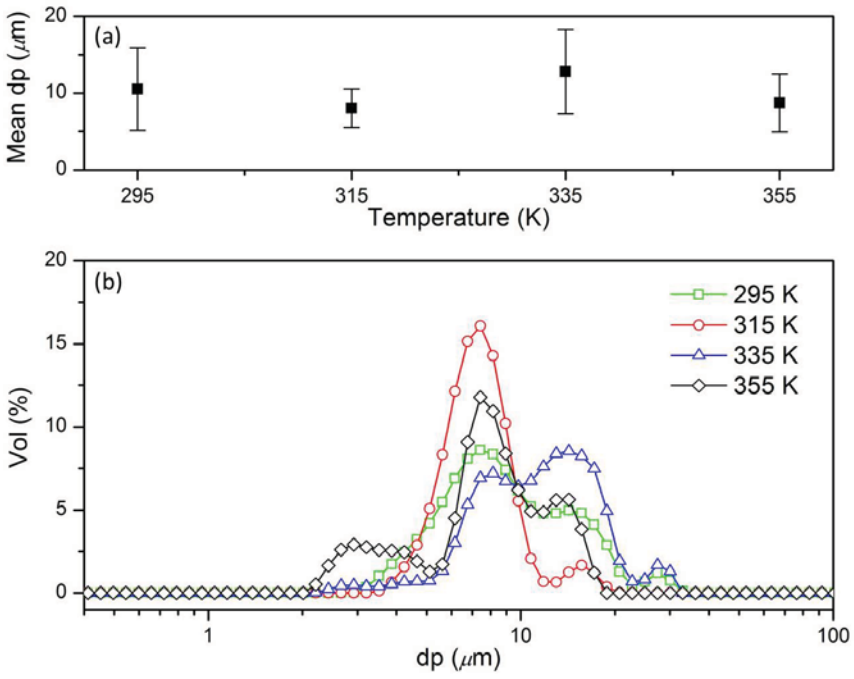

Figure 10. Mean particle size (a) and particle-size distributions (b) of $CaCO_3$, synthesized using model Ca-solution as a function of reaction temperature (aging time = 30 min).

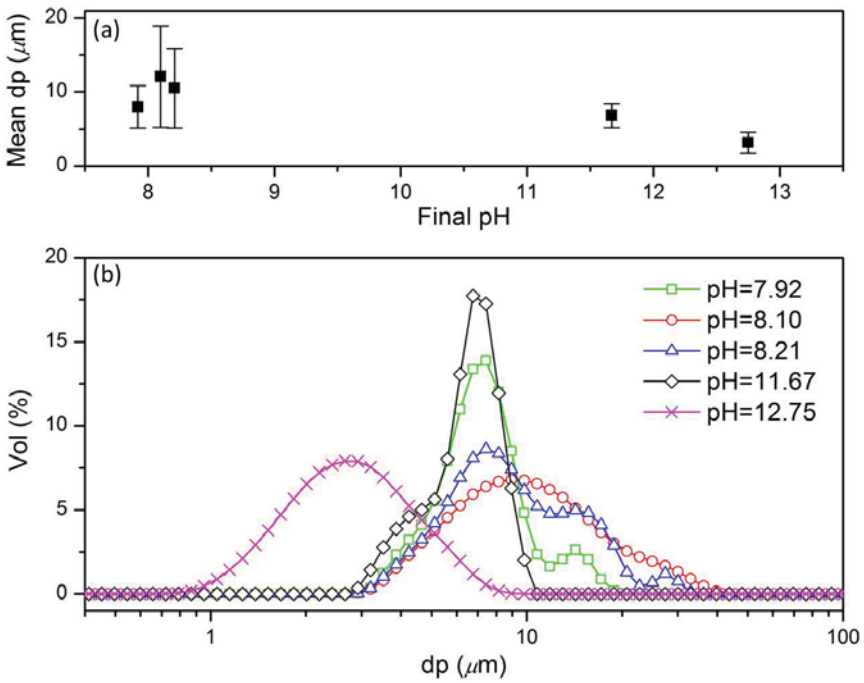

Figure 11. Mean particle size (a) and particle size distributions (b) of $CaCO_3$ synthesized using model Ca-solution as a function of pH at 295 K (aging time = 30 min, pH was measured after the precipitation)

3.2.2 Effects on Morphological Structure

The morphological structures of produced PCC particles were investigated using SEM. Figure 12 shows the effect of pH on the particle morphological structure. At low-pH conditions, the particles were spherical. At high-pH conditions, the morphological structure of particles changed to rosette-shaped, which have a larger surface area than the smooth, spherical particles. It is known that the spherical particles are suitable as paper fillers. The PCC produced at highest pH (12.75) was amorphous, and this explains the wide particle-size distribution observed during the particle-size analysis.

Figure 13 shows the effect of reaction temperature on the particle's morphological structure. At 295 K, the particles were spherical. When the temperature was increased to 315K, the structure started to change and became rosette-shaped. As the reaction temperature was further increased to 335K, the PCC particles changed to needle-like structure. As shown in both Figure 12 and Figure 13, the effect of reaction temperature was stronger than the effect of pH on the particle size and morphological structure. The effect of reaction time on the particle's morphological structure can be neglected.

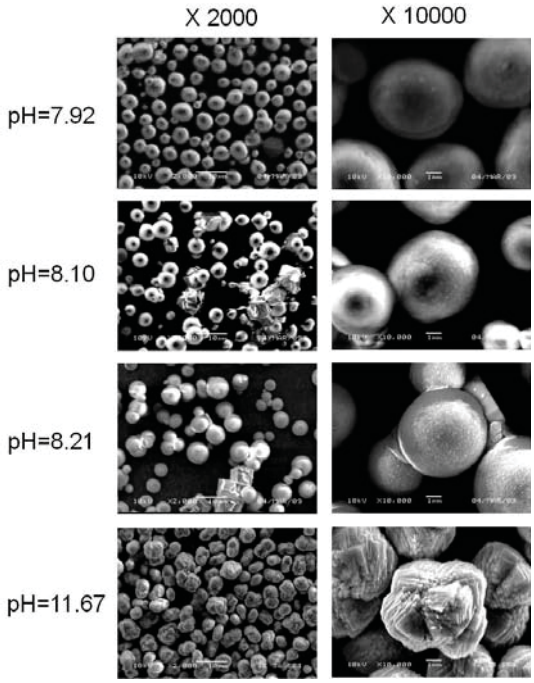

Figure 12. SEM images of $CaCO_3$ synthesized using model Ca-solution at various pH conditions (reaction temperature = 295 K, aging time= 30 min).

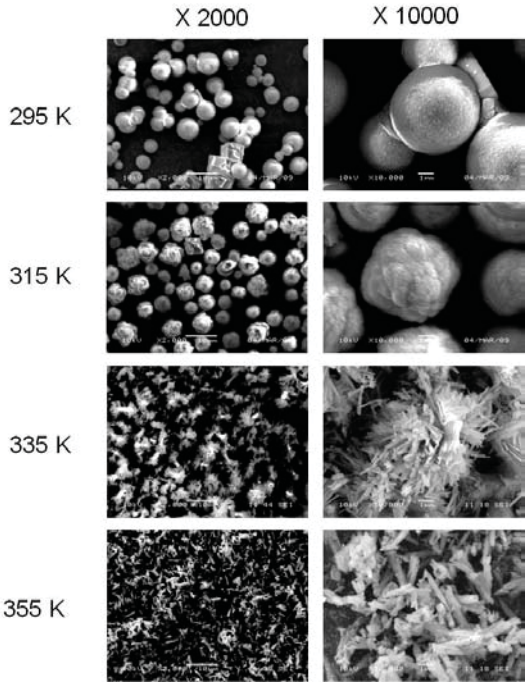

Figure 13. SEM images $CaCO_3$ synthesized using model Ca-solution at various temperature conditions (aging time =30 min).

3.2.3 Effects of Different Calcium Sources on Synthesis of Precipitated Calcium Carbonate

In order to estimate the possibility of using $CaCO_3$ synthesized with soluble Ca species extracted from wollastonite (denoted as $CaCO_3$(W)), its particle-size distribution and morphological structure were compared with the $CaCO_3$ synthesized with the pure chemical of $Ca(NO_3)_2$ (denoted as $CaCO_3$(M)). The $CaCO_3$ particles formed from two different Ca sources of wollastonite and $Ca(NO_3)_2$ were synthesized at the same temperature and pH conditions for comparison. Figure 14 shows the particle-size distributions of $CaCO_3$(W) and $CaCO_3$(M) at two different temperatures of 295 K and 355 K. As shown in Figure 14, the particle-size distributions at 295 K were quite similar. On the other hand, the patterns at 355 K were different. It was reported that the organic additives could affect the morphological structure of PCC.[49] Thus, the differences were attributed to the use of acetic acid to extract Ca from wollastonite.

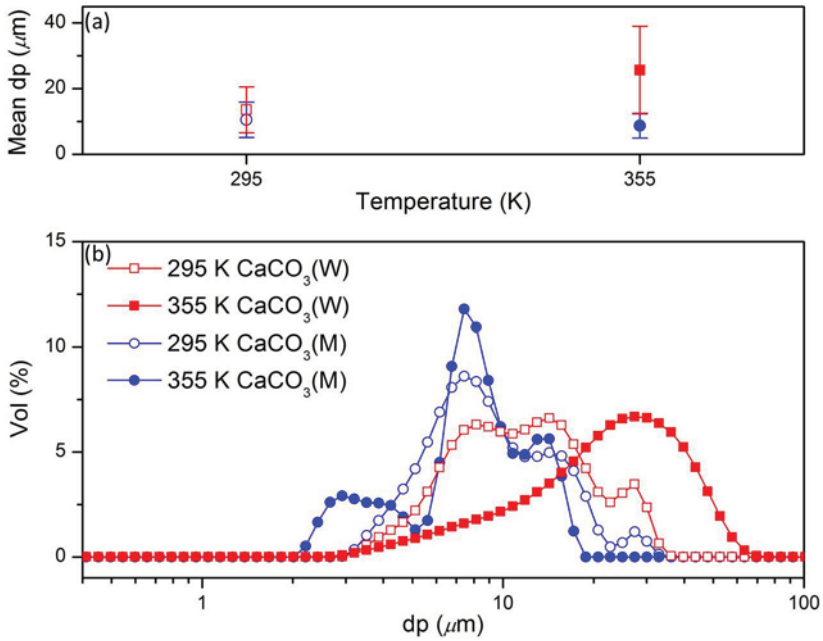

Figure 14. Comparison of mean particle size (a) and particle-size distributions (b) of $CaCO_3$, synthesized using wollastonite and model Ca-solution at 295 K and 355 K (aging time = 30 min)

XRD patterns were analyzed to determine the crystalline structures and compositions of synthesized PCC. Figure 15 shows XRD patterns of $CaCO_3$(W) and $CaCO_3$(M) synthesized at 297 K and 355 K, and their Rietveld refinement fits. As shown in Figure 15 (a), both $CaCO_3$(W) and $CaCO_3$(M) include two different crystalline structures of vaterite (space group: $P6_3/mmc$, a = 4.12 Å, c = 8.45 Å) and calcite (space group: $R\bar{3}c$, a = 4.99 Å, c = 17.05 Å). In the case of $CaCO_3$(W), the composition of calcite was 24 wt% with 76 wt% of vaterite, whereas $CaCO_3$(M) included calcite and vaterite of 33 wt% and 67 wt%, respectively. Because the vaterite is metastable, it is not only less common in nature, but also commercially a less significant polymorph of PCC. In contrast, calcite is the most common polymorph of PCC in commercial applications. At higher temperature of 355 K (Figure 15 (b)) both $CaCO_3$(W) and $CaCO_3$(M)

changed their polymorphic structures to aragonite (space group: Pnma, a = 4.95 Å, b = 7.96 Å, c = 5.74 Å) with a small amount of calcite ($CaCO_3$(W): 87 wt% of aragonite with 13 wt% of calcite, $CaCO_3$(M): 96 wt% of aragonite with 4 wt% of calcite). Aragonite was observed as a major polymorph of $CaCO_3$ at 355 K because a phase transition from vaterite to aragonite occurs above 330 K.[50]

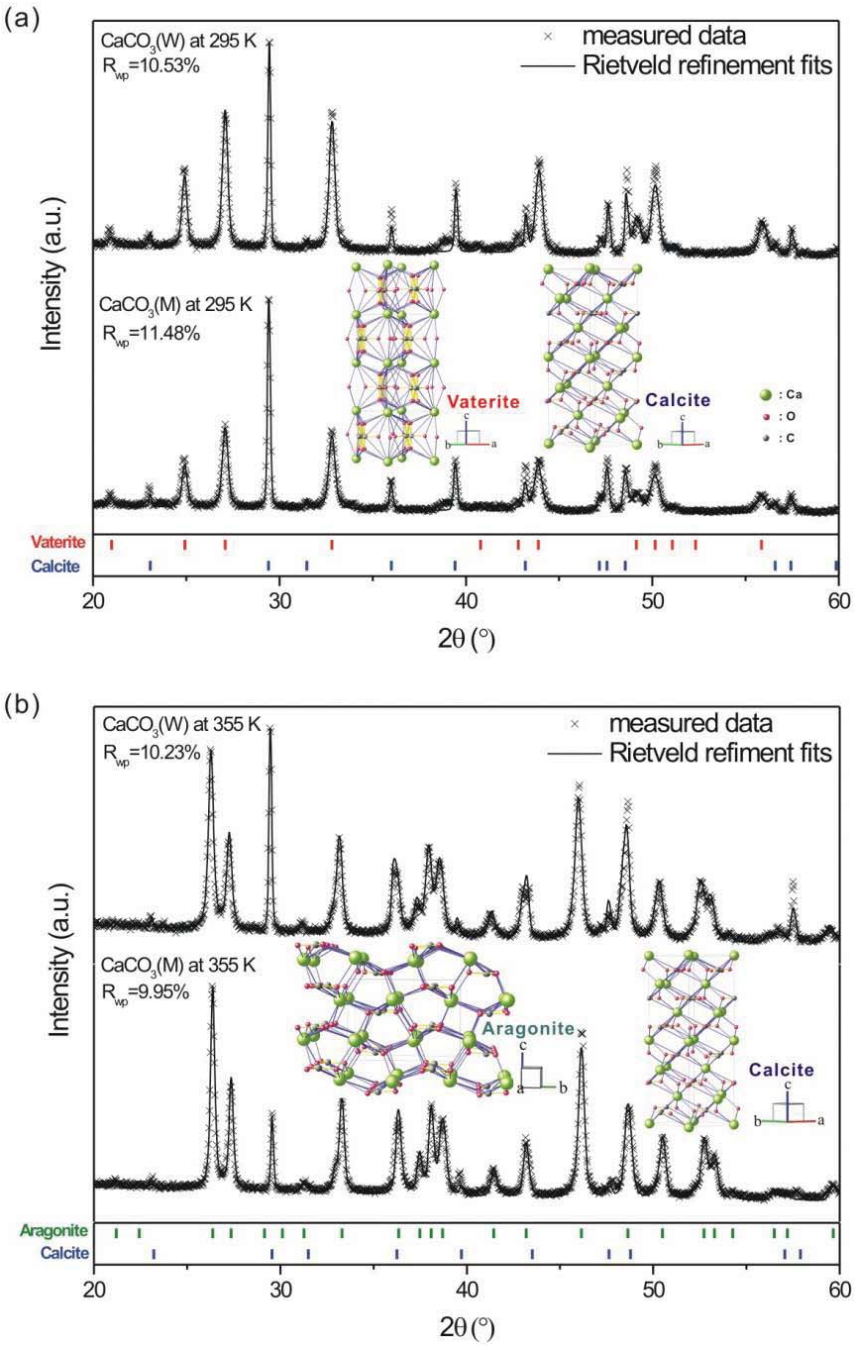

Figure 15. Rietveld refinement results of $CaCO_3$ synthesized with wollastonite and $Ca(NO_3)_2$ at (a) 295 K and (b) 355 K. Insets indicate crystalline the structures of vaterite, calcite, and aragonite.

Figure 16 shows a comparison of the morphological structures of $CaCO_3$(W) synthesized at 295 K and 355 K with $CaCO_3$(M). As shown in Figure 16 (a) and (b), $CaCO_3$ particles synthesized at 295 K exhibited spherical shapes, but the shape of synthesized PCC changed to needle-like at a higher reaction temperature (Figure 16 (c) and (d)). Generally, aragonite exhibits needle-shape orthorhombic structures, and the aspect ratio (length-to-diameter) is a very important property in many applications, particularly for aragonite. High aspect ratio in aragonite is suitable in applications that require high strength and incident light scattering.

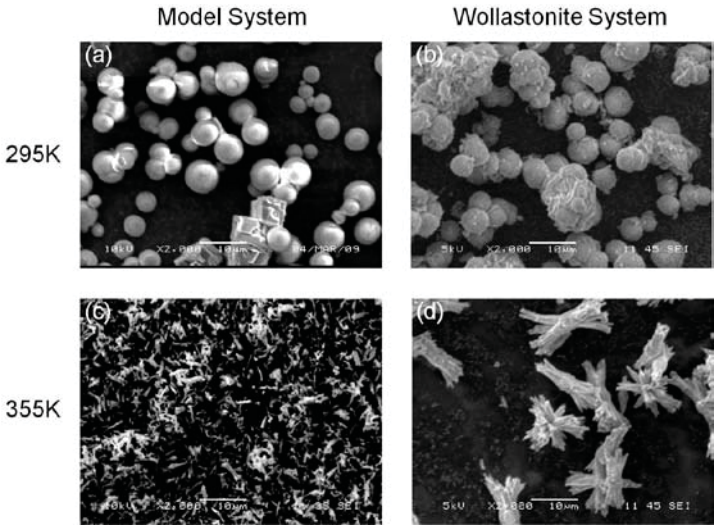

Figure 16. SEM images of $CaCO_3$ synthesized with $Ca(NO_3)_2$ ((a) and (c)) and wollastonite ((b) and (d)) at two temperature conditions, of 295 K and 355 K, with different magnifications.

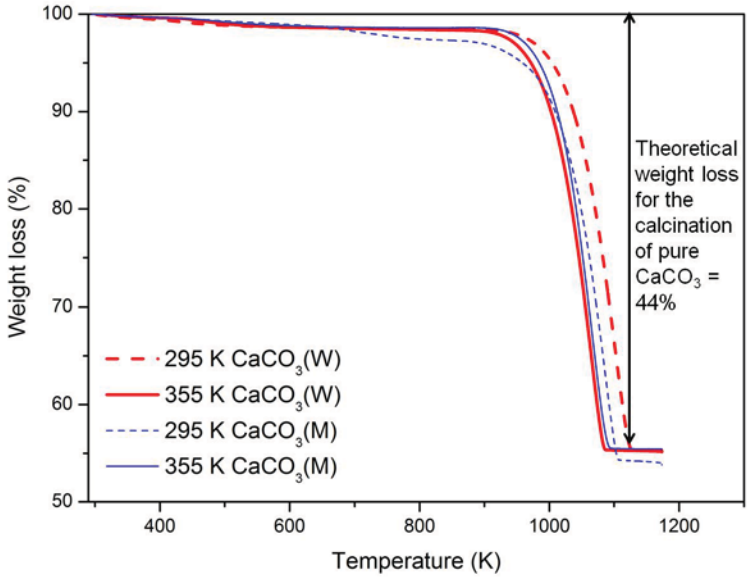

Figure 17. TGA results of $CaCO_3$ synthesized with wollastonite and $Ca(NO_3)_2$ at 295 K and 355 K.

There was no difference in the thermal stability among the PCC samples synthesized under different conditions. The weight loss for each PCC sample was a little higher than 44%, which is the theoretical weight loss for the calcination of pure $CaCO_3$ (Figure 17). The extra weight loss was attributed to the moisture in the PCC samples.

A comparison between PCC synthesized from wollastonite and $Ca(NO_3)_2$ revealed that their morphological and crystal structures were identical. Their structures could be controlled by changing the reaction parameters, such as temperature and pH. Further process optimization is required to produce uniform and highly specific PCC. Particularly, the effect of chelating agents on the particle distributions and morphology of PCC will be subjected to future investigations.

4 Thermodynamic Modeling and Flow Diagram of Industrial Process

4.1 Thermodynamic Modeling

Instead of using MATLAB to do the thermodynamic modeling of the H_2O-CO_2-CaO-SiO_2 system, a thermodynamic modeling of the H_2O-CO_2-wollastonite system was done using the software PHREEQCI. PHREEQCI is a Windows-based interface that provides access to all the capabilities of PHREEQC. PHREEQC is a computer program for simulating chemical reactions and transport processes in natural or polluted water. The program is based on equilibrium chemistry of aqueous solutions interacting with minerals, gases, solid solutions, exchangers, and sorption surfaces, but it also includes the capability to model kinetic reactions with rate equations that are completely user-specified in the form of Basic statements.[51]

PHREEQC is capable of simulating a variety of geochemical reactions for a system including:

- Mixing of waters,
- Addition of net irreversible reactions to solution,
- Dissolving and precipitating phases to achieve equilibrium with the aqueous phase, and
- Effects of changing temperature.

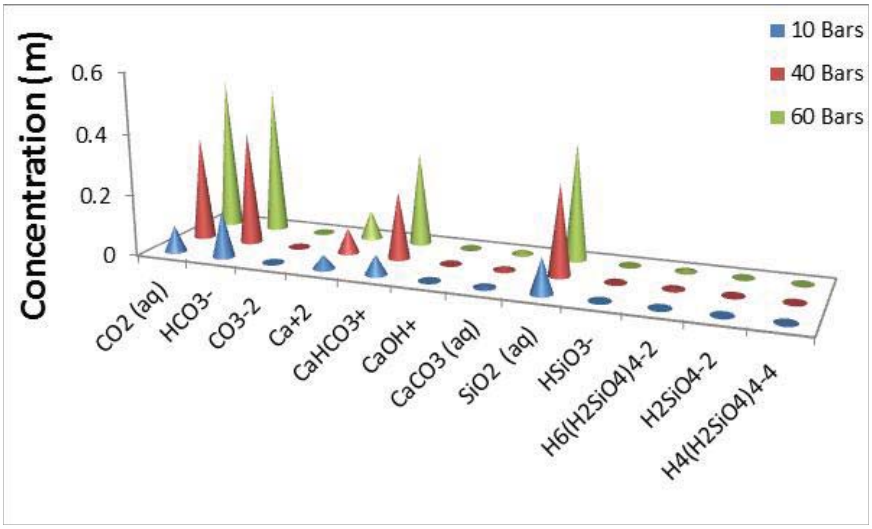

Figure 18. Effect of the partial pressure of CO_2 on wollastonite dissolution at 120 ºC.

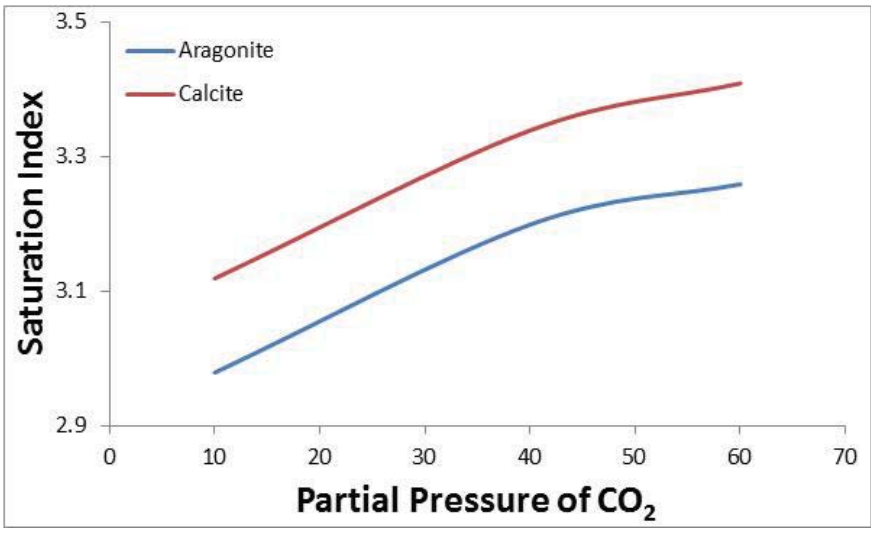

Figure 19. Effect of the partial pressure of CO_2 on precipitation of calcium carbonate at 120 ºC.

First, carbonation of excess wollastonite mineral in the water was simulated under various partial pressures of CO2 conditions (10 bars, 40 bars and 60 bars) at 120 °C (393 K). The simulation results were shown in Figure 18 and Figure 19. As shown in Figure 18, a higher partial pressure of CO2 resulted in a lower pH in the system, which consequently increased the dissolution of wollastonite. Both the pH and partial pressure of CO2 affect the precipitation of calcium carbonate. As shown in Figure 19, a higher partial pressure of CO2 increased the precipitation of calcium carbonate at 120 °C (393 K). This means that at 120 °C (393 K), the effect of CO2 partial pressure on the precipitation of calcium carbonate is bigger than the effect of the changing pH.

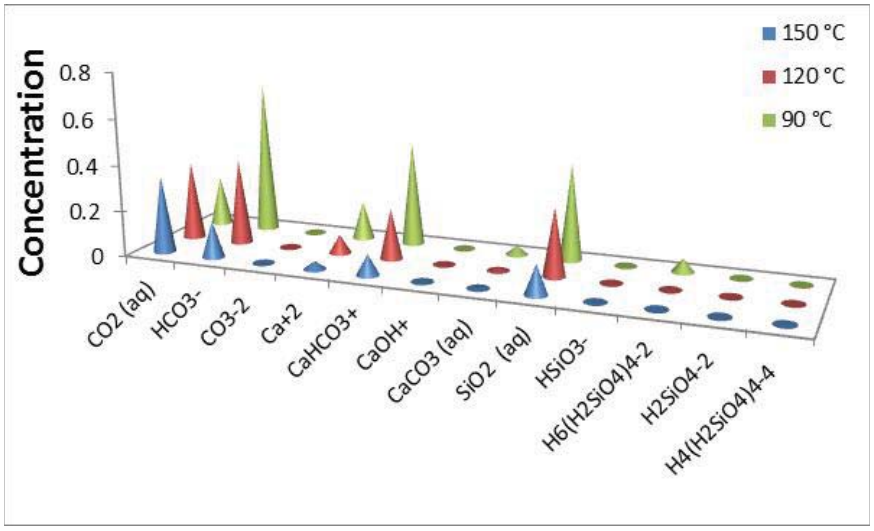

Figure 20. Effect of temperature on wollastonite dissolution at P_{CO2} = 40 bars.

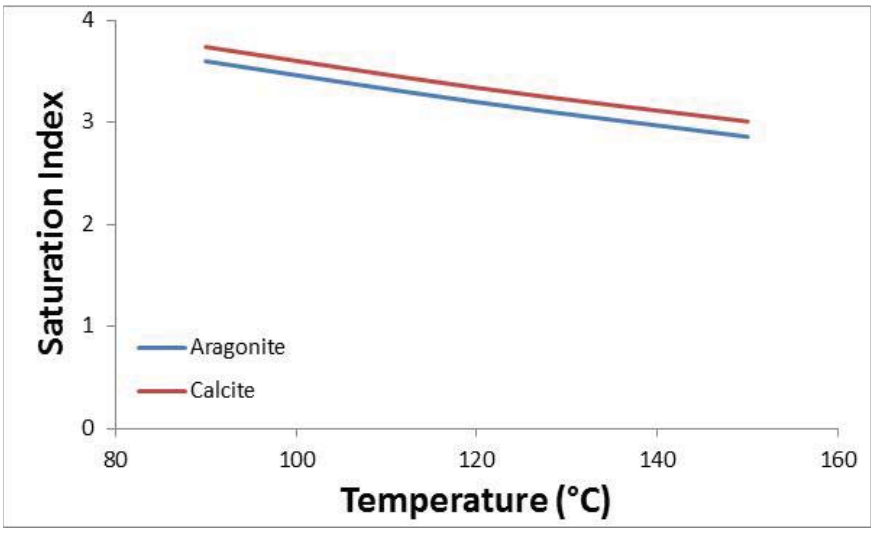

Figure 21. Effect of temperature on precipitation of calcium carbonate at P_{CO2} = 40 bars.

Then, carbonation of excess wollastonite mineral in the water was simulated under a constant partial pressure of CO2 (40 bars) at various temperature conditions (90 °C (363 K), 120 °C (393 K) and 150 °C (423 K)). As Figure 20 and Figure 21 show, increases in system temperature caused a decrease in the dissolution of wollastonite and precipitation of calcium carbonate, because the CO2 dissolution favors low temperature.

4.2 Flow Diagram of Industrial Process

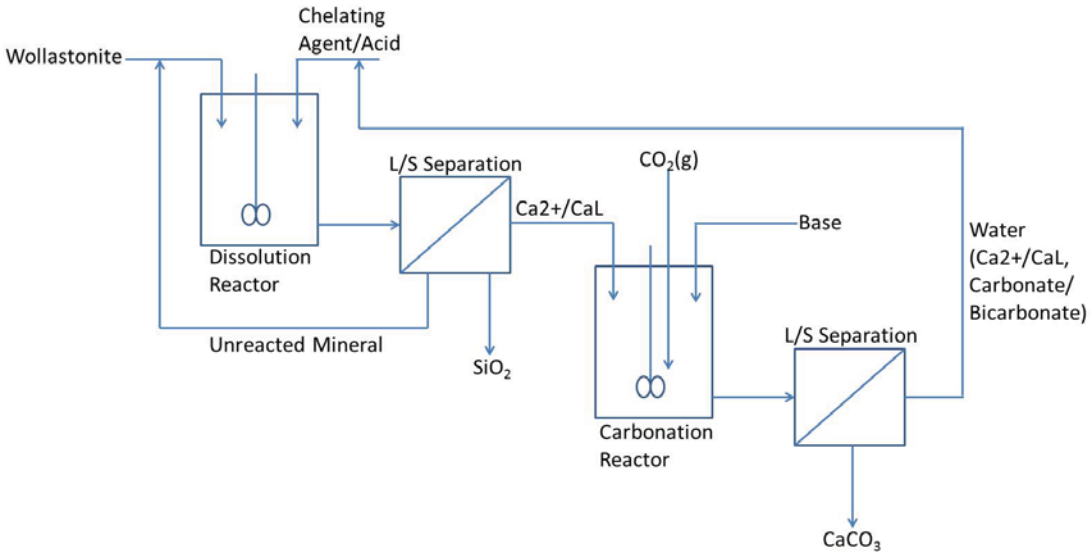

Figure 22. Sketch of flow diagram of the industrial carbon-mineralization process.

Figure 22 shows the sketch of a flow diagram of the industrial carbon-mineralization process with wollastonite. There are two main continuous stirred-tank reactors, one for wollastonite dissolution and

another for precipitation of calcium carbonate. 62.3% of calcium was leached out from wollastonite minerals in three hours in a laboratory experiment. The dissolution experiment was performed under ambient pressure with air in a batch reactor, and the reaction temperature was 80 °C (353 K). 1 M acetic acid was used as a chelating agent. Citric acid was also tested as a chelating agent for wollastonite dissolution, but it formed a gel-like material in the batch reactor and did not enhance the wollastonite dissolution.

Based on the batch dissolution experiments in the laboratory and thermodynamic modeling of the H_2O-CO_2-wollastonite system, the dissolution reactor can be operated around 90 °C (363 K) to get above 70% calcium recovery from wollastonite minerals with 1 M acetic acid in three hours. To get higher recovery of calcium from wollastonite, strong acid, such as HNO_3, can be added to decrease the pH in the dissolution reactor. Another option is to increase reaction temperature (around 120-150 °C (393-423 K)—considering the thermal and energy penalty, the temperature cannot be too high), but in this case the dissolution reactor cannot be operated under ambient pressure.

The carbonation reactor should be operated under high partial pressure of CO_2, with addition of a base to increase the pH (e.g. $NaHCO_3$, NaOH). The liquid solution from the dissolution reactor is acidic, and dissolution of CO_2 also decreases pH in the reactor. Since precipitation of calcium carbonate is favored at high pH, a base should be added to increase the pH in the carbonation reactor. Precipitation of calcium carbonate also favors low temperature, but when considering the kinetics, the reaction temperature should not be lowered very far. In addition, the product morphology can be selected with temperature. To get vaterite and calcite as final products, operation temperature should be lower than 330 K; to get aragonite and calcite as final products, operation temperature should be higher than 330 K.

References

1. IPCC (Intergovernmental Panel on Climate Change), *Climate Change 2007: Synthesis Report*, Cambridge Univ. Press: New York, **2007**.

2. IPCC (Intergovernmental Panel on Climate Change), *Carbon Dioxide Capture and Storage*, Cambridge Univ. Press: New York, **2005**.

3. CCSP (U.S. Climate Change Science Program and the Subcommittee on Global Change Research), *Abrupt Climate Change: Final Report*, U.S. Geological Survey, Reston, VA, **2008**.

4. IEA, World Energy Outlook 2010, Organization for Economic Co-operation and Development, **2010**.

5. Lackner, K. S. A guide to CO_2 sequestration. *Science* **2003**, *300*, 1677−1678.

6. Haszeldine, R. S. Carbon capture and storage: how green can back be? *Science* **2009** , *325*, 1647−1652.

7. Holloway, S. Storage of fossil fuel-derived carbon dioxide beneath the surface of the earth. *Annu. Rev. Energy Environ*. **2001**, *26*, 145−166.

8. Orr. F. M., Jr. Onshore geologic storage of CO_2. *Science* **200**9, *325*, 1656−1658.

9. Brewer, P. G.; Friederich, G.; Pelzer, E. T.; Orr. F. M., Jr. Direct experiments on the ocean disposal of fossil fuel CO_2. *Science* **1999** , *284*, 943−945.

10. Martin, J. H.; Coale, K. H.; Johnson, K. S.; Fitzwater, S.; Gordon, R. M.; Tanner, S. J.; Hunter, C. N.; Elrod, V. A.; Nowickl, J. L.; Coley, T. L.; Barber, R. T.; Lindley, S.; Watson, A. J.; van Scoy, K.; Law, C. S.; Liddicoat, M. I.; Ling, R.; Stanton, T.; Stockel, J.; Collins, C.; Anderson, A.; Bidigare, R.; Ondrusek, M.; Latasa, M.; Millero, F. J.; Lee, K.; Yao, W.; Zhang, J. Z.; Freiderich, G.; Sakamoto, C.; Chavez, F.; Buck, K.; Kolber, Z.; Greene, R.; Falkowski, P.; Chisholm, S. W.; Hoge, F.; Swift, R.; Yungel, J.; Turner, S.; Nightingale, P.; Hatton, A.; Liss, P.; Tindale, N. W. Testing the iron hypothesis in ecosystems of the equatorial Pacific Ocean. *Nature* **1994**, *371*, 123−129.

11. Seifritz, W. CO_2 disposal by means of silicates. *Nature* **1990**, *345*, 486.

12. Fan, L.-S.; Park, A.-H. A.; Lackner, K. S. Carbon dioxide capture and disposal: carbon sequestration. In *Encyclopedia of Chemical Processing*; Lee, S. Ed.; CRC Press: Boca Raton, FL **2005**; pp 305.

13. Park, A.-H. A.; Lackner, K. S.; Fan, L.-S. Carbon Sequestration. In *Hydrogen Fuel: Production, Transport and Storage*; Gupta, R. Ed.; CRC Press: Boca Raton, FL **2008**; pp 569.

14. Zevenhoven, R; Fagerlund, J. Fixation of CO_2 into inorganic carbonates: the natural and artificial "weathering of silicates". In *Carbon Dioxide as Chemical Feedstock*; Aresta, M. Ed.; Wiley VCH Verlag: Germany **2010**; pp 353.

15. Kojima, T.; Nagamine, A; Uemiya, S. Absorption and fixation of carbon dioxide by rock weathering. *Energ Convers. Manage*. **1997**, *34*, 461−466.

16. Gunter, W. D.; Perkins, E. H.; McCann, T. J. Aquifer disposal of CO_2 rich gases: reaction design for added capacity. *Energ Convers. Manage*. **1993**, *34*, 941−948.

17. Butt, D. P.; Lackner, K. S.; Wendt, C. H.; Vaidya, R.; Piled, L; Park, Y.; Holesinger, T.; Harradine, D. M.; Nomura, K. The kinetics of binding carbon dioxide in magnesium carbonate. In *Proceedings of the 23rd International Technical Conference on Coal Utilization and Fuel Systems*, March 9−13, **1998**. Clearwater, FL.

18. Lackner, K. S.; Butt, D. P.; Wendt, C. H. Progress on binding CO_2 in mineral substrates. *Energ Convers. Manage*. **1997**, *38*, 259−264.

19. Newall, P. S.; Clarke, S. J.; Haywood, H. M.; Scholes, H.; Clarke, N. R.; King, P. A.; Barley, R. W. *CO_2 storage as carbonate minerals*, Report number PH3/17; IEA Greenhouse Gas R&D Pro-gramme; pp. 185, **2000**.

20. Zevenhoven, R.; Fagerlund, J.; Songok, J. K. CO_2 mineral sequestration: developments toward large-scale application. *Greenhouse Gas Sci Technol*. **2011**, *1*, 48−57.

21. O'Connor, W. K.; Dahlin, D. C.; Nilsen, D. N.; Walters, R. P.; Turner, P. C. Carbon dioxide sequestration by direct mineral carbonation with carbonic acid. In *Proceedings of the 23rd International Technical Conference on Coal Utilization and Fuel Systems*; March 9−13, **1998** Clearwater, FL.

22. O'Connor, W. K.; Dahlin, D. C.; Rush, G. E.; Gerdemann, S. J.; Penner, L. R.; Nilsen, R. P. *Aqueous Mineral Carbonation: Mineral Availability, Pretreatment, Reaction Parametrics, and Process Studies*; DOE/ARC-TR-04-002; Albany Research Center: Albany, OR, **2005**.

23. Gerdemann, S. J.; O'Connor, W. K.; Dahlin, D. C.; Penner, L. R.; Rush, H. Ex situ aqueous mineral carbonation. *Environ. Sci. Technol*. **2007**, *41*, 2587−2593.

24. Kakizawa, M.; Yamasaki, A.; Yanagisawa, Y. A new CO_2 disposal process via artificial weathering of calcium silicate accelerated by acetic acid. *Energy* **2001**, *26*, 341−354.

25. Park, A.-H. A.; Fan, L. CO_2 mineral sequestration: physically activated dissolution of serpentine and pH swing process. *Chem. Eng. Sci*. **2004**, *59*, 5241−5247.

26. Maroto-Valer, M. M.; Fauth, D. J.; Kuchta, M. E.; Zhang, Y.; Andresen, J. M. Activation of magnesium rich minerals as carbonation feedstock materials for CO_2 sequestration. *Fuel Process Technol*. **2005**, *86*, 1627−1645.

27. Jarvis, K.; Carpenter, R. W.; Windman, R.; Kim, Y.; Nunez, R.; Alawneh, F. Reaction mechanism for enhancing mineral sequestration of CO_2. *Environ. Sci. Technol*. **2009** , *43*, 6314−6319.

28. Hanchen, M; Prigiobbe, V.; Storti, G.; Seward, T. M.; Mazzotti, M. Dissolution kinetics of fosteritic olivine at 90−150 °C including effects of the presence of CO_2. *Geochim. Cosmochim. Ac.* **2006**, *70*, 4403−4416.

29. Hanchen, M.; Krevor, S.; Mazzotti, M.; Lackner, K. Validation of a population balance model for olivine. *Chem. Eng. Sci*. **2007**, *62*, 6412−6422.

30. Krevor, S. C.; Lackner, K. S. Enhancing process kinetics for mineral carbon sequestration. *Energy Procedia* **2009**, *1*, 4867−4871.

31. Prigiobbe, V.; Hanchen, M.; Werner, M.; Baciocchi, R.; Mazzotti, M. Mineral carbonation process for CO_2 sequestration. *Energy Procedia* **2009**, *1*, 4885−4890.

32. Goff, F.; Lackner, K. S. Carbon dioxide sequestering using ultramafic rocks. *Environ. Geosci*. **1998**, *5*, 89−101.

33. Oelkers, E. H.; Gislason, S. R.; Matter, J. Mineral carbonation of CO_2. *Elements*, **2008**, *4*, 333− 337.

34. Singer, D. A.; Menzie, W. D. *Quantitative mineral resource assessments− an integrated approach* ; Oxford University Press: Oxford, U. K., **2010**.

35. U.S. Geological Survey, Mineral Commodity Summaries, **2011**.

36. Huijgen, W. J. J.; Witkamp, G. J.; Comans, R.NJ Mineral CO_2 sequestration by steel slag carbonation. *Environ. Sci. Technol*. **2005**, *39*, 9676–9682.

37. Teir, S.; Eloneva, S.; Fogelholm, C. J.; Zevenhoven, R. Dissolution of steelmaking slags in acetic acid for precipitated calcium carbonate production. *Energy* **2007**, *32*, 528–539.

38. Iizuka, A.; Fujii, M.; Yamasaki, A.; Yanagisawa, Y. Development of a new CO_2 sequestration process utilizing the carbonation of waste cement. *Ind Eng Chem Res* **2004**, *43*, 7880–7887.

39. Huntzinger, D. N.; Gierke, J. S.; Kawatra, S. K.; Eisele, T. C.; Sutter, L. L. Carbon dioxide sequestration in cement kiln dust through mineral carbonation. *Environ. Sci. Technol.* **2009**, *43*, 1986–1992.

40. U.S. Geological Survey, Wollastonite- A Versatile Industrial Mineral, **2001**.

41. Lazzeri, A., S.M. Zebarjad, M. Pracella, K., Cavalier, and R. Rosa. Filler toughening of plastics. Part 1. – The effect of surface interactions on physico-mechanical properties and rheological behavior of ultrafine $CaCO_3$/HDPE nanocomposites. *Polymer.* ***2005***, 46(3), 827-844.

42. Miller, M. Lime. In *2005 Minerals Yearbook*. US department of the interior and US geological survey. **2006**. 44.1-44.14.

43. Teir, S.; Eloneva, S.; Zevenhoven, R. Production of precipitated calcium carbonate from calcium silicates and carbon dioxide. *Energ Convers. Manage.* **2005**, *46*, 2954–2979.

44. Specialty Minerals. Albacar 5970 Dry PCC. In *Performance Minerals for Paper Technical Data.* Bethlehem, PA. **2003**.

45. Lutterotti, L.; Matthies, S.; Wenk, H.-R.; Schultz, A. S.; Richardson, J. W. Combined texture and structure analysis of deformed limestone from time-of-flight neutron diffraction spectra. *J. Appl. Phys*. **1997**, *81*, 594–600.

46. Cyrus Feldman. Behavior of trace refractory minerals in the lithium metaborate fusion-acid dissolution procedure. *Analytical Chemistry*. **1983**, 55 (14), 2451–2453.

47. Gajewski, M.; Klobukowski, M. DFT studies of complexes between ethylenediamine tetraacetate and alkali and alkaline earth cations. *Can. J. Chem*. **2009** , *87*, 1492–1498.

48. Morel, F.; Hering, J. In *Principles and applications of aquatic chemistry*. Wiley-Interscience, **2003**.

49. Park, W. K.; Ko, S.-J.; Lee, S. W.; Cho, K.-H.; Ahn, J.-W.; Han, C. Effects of magnesium chloride and organic additives on the synthesis of aragonite precipitated calcium carbonate. *J. Crystal Growth*. **2008**, *310*, 2593–2601.

50. Fuchigami, K.; Taguchi, Y.; Tanaka, M. Synthesis of calcium carbonate vaterite crystals and their effect on stabilization of suspension polymerization of MMA. *Adv. Powder Technol.* **2009**, *20*, 74–79.

51. U.S. Department of the interior and U.S. geological survey, User's guide to PHREEQC. 1999

NYSERDA, a public benefit corporation, offers objective information and analysis, innovative programs, technical expertise and funding to help New Yorkers increase energy efficiency, save money, use renewable energy, and reduce their reliance on fossil fuels. NYSERDA professionals work to protect our environment and create clean-energy jobs. NYSERDA has been developing partnerships to advance innovative energy solutions in New York since 1975.

To learn more about NYSERDA programs and funding opportunities visit nyserda.ny.gov

New York State Energy Research and Development Authority

17 Columbia Circle
Albany, New York 12203-6399

toll free: 1 (866) NYSERDA
local: (518) 862-1090
fax: (518) 862-1091

info@nyserda.ny.gov
nyserda.ny.gov

Disposing of Greenhouse Gases through Mineralization Using the Wollastonite Deposits of New York State

Final Report
May 2012

State of New York
Andrew M. Cuomo, Governor

New York State Energy Research and Development Authority
Francis J. Murray, Jr., President and CEO